Lighting up dark exomoons: observational signatures of tidally induced volcanism in other worlds

Kleisioti, E.

1 | Introduction

1.1 Introduction

All gas giant planets in our Solar System are orbited by moons. Jupiter alone hosts nearly 90, while Saturn has more than 200 natural satellites (NASA Planetary Data System, 2025). Even some rocky planets have moons, such as the Earth with our Moon, Mars accompanied by two known moons, and Pluto, a rocky dwarf planet, which hosts five moons, as of the time of writing (NASA Planetary Data System, 2025). These natural satellites exhibit remarkable diversity in size, and surface properties, as can be seen in Figure 1.1, orbital characteristics, composition, interior structures, and the presence or absence of atmospheres.

The moons of the Solar System represent extremes of planetary science: Io, a Jovian satellite, is the most volcanically active body in the Solar System, with over 150 hotspots on its surface (Davies et al., 2015). Meanwhile, the majority of the large moons contain a significant amount of water ice. These -so called- icy moons display a wide range of sizes and characteristics themselves. For instance, even though most of them lack a dense, bound atmosphere, Titan, a large moon of Saturn, stands out. Titan possess a dense methane-rich atmosphere and lakes of liquid ethane and methane. The surfaces of icy moons are cold and icy, and a large number of them, such as Titan, Enceladus and Triton among others, are thought to sustain subsurface water oceans (Soderlund et al., 2024). The rest of the large moons in our Solar System consist mostly of rocky material; examples are Io, and our own Moon. Together, these natural satellites highlight the variety of environments found within our Solar System.

Scientific interest in exploring the moons of our Solar System has grown, particularly following the landmark Voyager 1 and 2 missions. These missions revolutionized our understanding of the outer Solar System by exploring the Jovian and Saturnian systems, including the discovery of active volcanoes on Io (Morabito, 2012). Subsequent missions have built on this foundation. Galileo revealed that Jupiter's icy moon Europa likely harbors a subsurface ocean (Khurana et al., 1998). Cassini uncovered evidence that Saturn's icy moon Enceladus possesses active plumes of water vapor (Dougherty et al., 2006). Before Cassini's observations, Enceladus was thought to be relatively unremarkable, and it was later revealed to host active plumes and a global subsurface ocean (McKinnon, 2015). Juno, focusing on Jupiter, continues to study the Jovian moons and their environment. The recent launches of ESA's JUICE (Jupiter Icy Moons Explorer) and NASA's Europa Clipper underline the high priority placed on exploring icy moons. For instance, Enceladus remains a high priority target for astrobiological studies, as highlighted by ESA's mission priorities in 2024 (Martins et al., 2025). NASA's 2023-2032 decadal strategy likewise emphasizes ocean worlds among the next decade's priority targets (National Academies of Sciences &Medicine, 2023). These missions and the study of moons will play a critical role in advancing our understanding of planetary systems and the potential for life beyond Earth.

One mechanism that plays an important role on the evolution and the current state

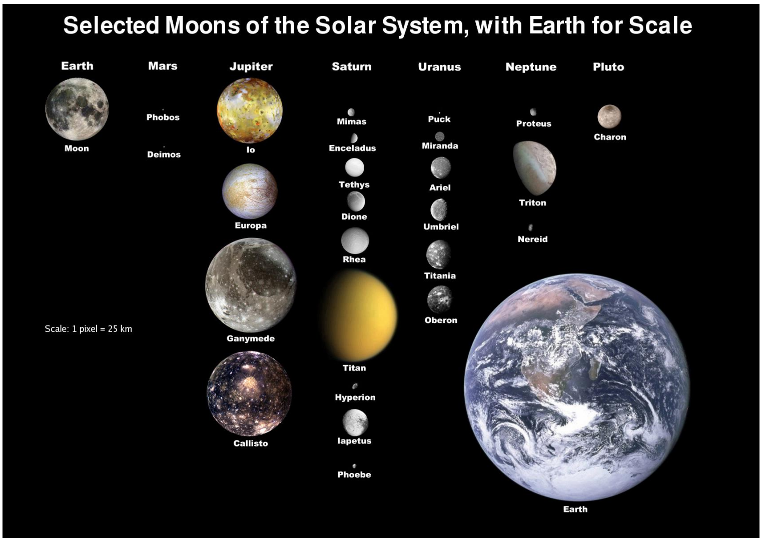

Figure 1.1: The moons of the Solar System show great diversity, in terms of size and composition. The Earth is presented for scale. Image courtesy of NASA

of surface and internal features in satellites is tidal dissipation, caused by tidal forces. A body's response to tidal forces is influenced by various factors, including its orbital parameters. For non-zero eccentricity orbits, tidal forces become stronger when the body is closest to its primary. This causes changes in the tidal bulge throughout the orbit, which generates internal friction and, subsequently, contributes to heating the interior. Tides can significantly influence the formation and maintenance of subsurface oceans, which are crucial for astrobiology, in the interior of moons. In addition, tides drive the extreme temperatures of Io (Segatz et al., 1988), and cryovolcanic plumes, like in the case of Enceladus (Terrile &Cook, 1981).

Moving outside of the Solar System, over the past two decades, more than 5,700 exoplanets have been discovered. Given the prevalence of moons in our Solar System, it is reasonable to expect that exoplanets also host natural satellites (exomoons). Beyond their potential astrobiological significance, the discovery and study of exomoons could provide valuable insights into planetary system formation and evolution, architectures, as well as population dynamics. Yet no exomoon detection has been confirmed, despite extensive searches (Teachey, 2024). With the launch of the JWST looking at the cosmos in infrared wavelengths, the natural question would be to see whether hot moons - from tidal heating, similar to Io - can be detected. And if so, what are the conditions that would make such a detection feasible.

In the following sections I introduce the different proposed exomoon detection methods, placing them in the context of exoplanet detection. In addition, I discuss tidal heating, its implications for Solar System moons, and how it affects our hunt to find moons outside of the Solar System.

1.2 Detecting extrasolar worlds

The discovery of two planets around the pulsar PSR1257 + 12 (Wolszczan &Frail, 1992), and the subsequent discovery of 51 Pegasi b, the first exoplanet discovered orbiting a main-sequence star (Mayor &Queloz, 1995) initiated an enormous growth of the invetory of known exoplanets that occurred over the last two decades. A diverse population of over 5,700 exoplanets has been currently identified, many of which bear little resemblance with the planets of our own Solar System. For example, 51 Pegasi b raised many questions in the scientific community, as it has a mass similar to that of Jupiter and an orbital period of just 4.2 days. Later it would turn out that these planets, named hot-Jupiters, are not uncommon. Currently one of the most common known planet type in our Galaxy is foreign to our Solar System; they have a size between that of the Earth and Neptune and are called super-Earths (Cloutier, 2024). On the contrary, Earth-sized planets represent only a small portion of the planets discovered so far. If the right conditions are met and they are distant enough from their star for water to remain in solid form, these planets can resemble the icy moons of our Solar System. These cold, ocean worlds are the topic of Chapter 5 of this thesis.

The field of exoplanets gives us the capability to place our Solar System and the Earth in the broader context of the population of other planetary systems. We are now at a stage where we can characterize exoplanet atmospheres by detecting molecules, like water, and study their atmospheric dynamics and clouds (see e.g. Helling (2019)). Additionally, by combining measurements of planets' mass and radii we can measure their bulk density, investigate their interior structures by modelling different material compositions, and assess their habitability potential. For this thesis, we are now pushing the boundaries of observational techniques in an effort to detect moons orbiting them. In the following section I will give a brief introduction on exoplanet detection methods, to provide the bases of understanding exomoon detection methods, discussed in Section 1.2.2.

1.2.1 Exoplanet detection methods

Indirect methods

Most of currently known exoplanets have been detected via indirect methods of detection. Their presence is inferred through an effect that they have on their stellar host's signal. The most successful of these methods are the transit and radial velocity methods (RV). Other indirect methods include microlensing, where the light of a distant background star is gravitationally influenced by the presence of the detected planet.

The transit method has been the most successful in finding exoplanets. Particularly, the number of detected transiting exoplanets exploded with the Kepler (Borucki et al., 2010), and TESS (Ricker et al., 2015) missions, which performed accurate photometry of a large number of stars and obtain their lightcurves, a measure of brightness over time. The method is based on detecting the dip caused by an orbiting planet in the lightcurve of their host star. The size of the dip gives the planets radius as a fraction of the star's one, and the time between two consequent transits, is a measure of the orbital period. This method is biased for exoplanets with small orbital periods, as close-in exoplanets com-

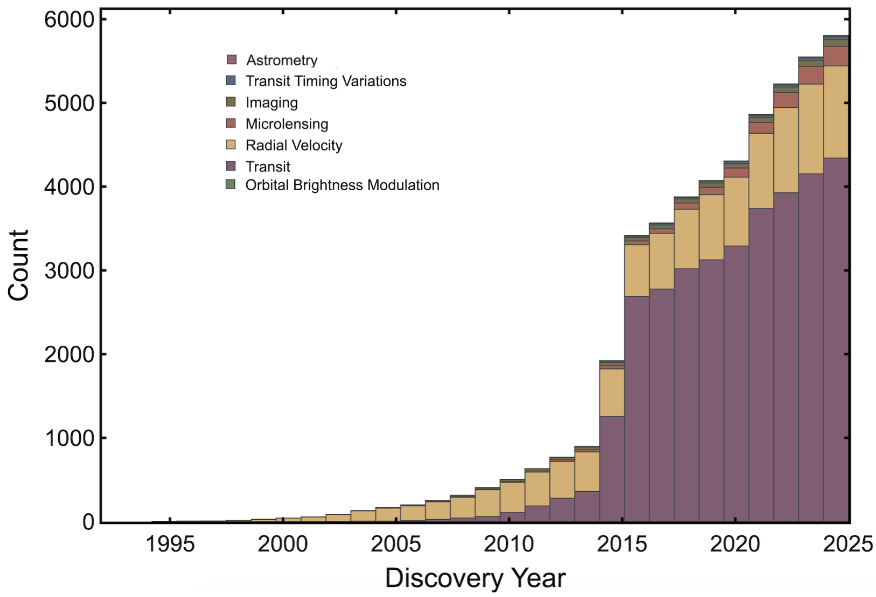

Figure 1.2: Known exoplanets as of March 2025. The graph shows the cumulative distribution of detected exoplanets per year and discovery method. Credit: NASA Exoplanet Archive

plete more transits in a given observation time, but also have higher transit probabilities. An important transiting system is the planet system of Trappist-1, which consists of seven Earth sized planets orbiting an M-dwarf (Gillon et al., 2017). It is the first known system of potentially rocky, terrestrial exoplanets with incident fluxes similar to those of the rocky planets in our Solar System. Three of the Trappist-1 planets lie within the star's habitable zone (HZ), which is the distance from the host star where water can exist in liquid form. As the light from the star passes through the planet's atmosphere during the transit, it gets absorbed at different wavelengths, depending on the atmosphere's chemical composition. When measuring the transit depth at different wavelengths, we can obtain the transmission spectrum of an exoplanet. This method is called transmission spectroscopy and gives the possibility to detect specific chemical compounds in the atmosphere, like H_2O (Tsiaras et al., 2019), and CO_2 (Ahrer et al., 2023).

The RV method measures variations in the Doppler shift of the star's spectrum, caused by the presence of an orbiting planet. The method is more sensitive to close-in, massive planets, as the shift in frequency of the spectral features of a planets is larger for more massive planets. The RV method provides us with the lower limit to the planet's mass and its orbital period. When this technique is combined with the transit method, astronomers can measure the bulk density of a planet. Initially the RV method was mostly sensitive to close-in massive planets (like 51 Pegasi b), however modern instruments can detect rocky planets around low mass stars (Suárez Mascareño et al., 2023). Two examples of planets discovered with the RV method, and discussed in this thesis are ϵ Eridani b (Hatzes et al., 2000) - Chapter 2, ϵ Indi A b (Feng et al., 2018) - Chapter 3.

Another exoplanet detection method is astrometry, where precise measurements of the perturbation of the linear motion of a star, due to the planet's orbit are taken. Astrometry is sensitive to planets with longer orbital periods, as such planets induce larger displacements in their star's position over the course of their orbit. This method has not been as successful as the transit and RV methods in detecting planets, and has resulted in only a handful of detections, as of March 2025. Apart from the high precision requirements that a detection requires, the bias for long period planets necessitates longer observation times (Endl &Cochran, 2007). In addition However, the Gaia mission and its upcoming Data Releases is expected to significantly increase that number (Espinoza-Retamal et al., 2023). Gaia scans the sky taking precise astrometric measurements of stars. Figure 1.2 shows the cumulative distribution of detected exoplanets per year and discovery method as of 2025 for each detection method.

Direct imaging

In contrast to the successful transit and RV methods, 83 exoplanets have been discovered via direct imaging (DI) (see Chauvin, 2024, for an extensive overview). Direct imaging works by suppressing the starlight to reveal the planet's flux. Spatially resolving the planet from the star in this context is challenging, as it requires to tackle the big contrast of the planet with respect to the star, particularly for close-in planets. This is why DI is relatively easier at larger angular separations. Although DI has resulted in relatively few discoveries, the method captures light directly from the planets, rather than merely inferring their presence. This comes with several advantages, as it can allow atmospheric characterization particularly for planets that are far from their stars, where other methods struggle. DI is also sensitive to detecting young exoplanets that are IR-bright and warm from their formation. In addition, unlike the transit method, which requires the orbit of the planet to pass in front of the disk of the star, DI can detect planets regardless of their orbital inclination, which in this context describes the angle between the plane of the orbit relative to the plane of the sky. However, planets on a highly inclined orbits are likely to experience close encounters with the star in the image plane, making detection more challenging. Some directly imaged systems include PDS 70 (two accreting protoplanets), in which a moon-forming disk was directly imaged for the first time (Benisty et al., 2021), and HR 8799 which hosts four wide-orbit giant planets (Marois et al., 2010). Both of these systems can be seen in Figure 1.3. Another notable system is that of YSES-1, which is the first directly imaged planet system around a Sun-like star, with multiple planets (Bohn et al., 2020). In the near future, the combination of adaptive optics and coronagraphs with next-generation large telescopes, such as the ELT, will enable DI and characterization of Earth-like planets (Snellen et al., 2015).

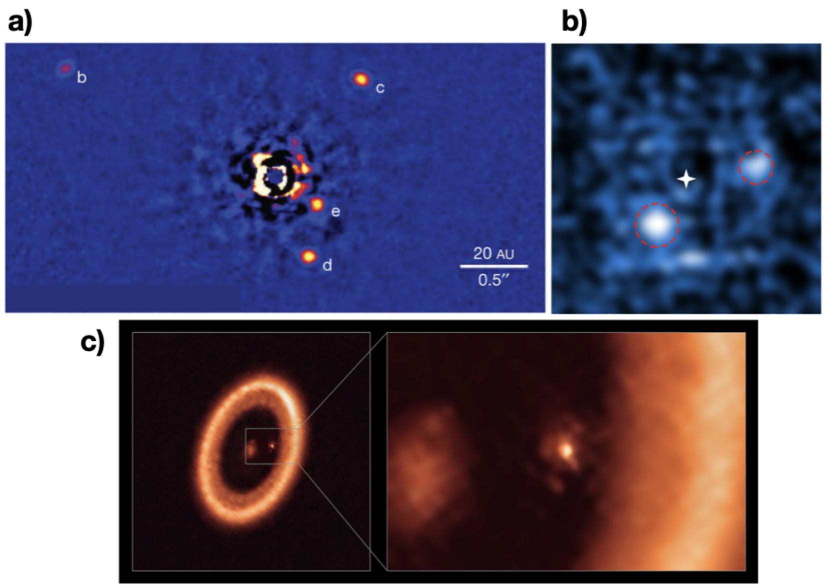

Figure 1.3: Several directly imaged planetary systems. a) The HR 8799 system (Marois et al., 2010) b) The planets PDS 70 b,c (Haffert et al., 2019) c) The circumplanetary disk around PDS 70c (Benisty et al., 2021)

1.2.2 Exomoons and their detection methods

Since every giant planet in the Solar System has a system of moons, it is plausible that exoplanets also host exomoons. While detection methods have become increasingly effective at identifying exoplanets, finding exomoons remains more difficult due to the subtle effects they have on an exoplanet's signal. However, advances in observational astronomy have already identified multiple exomoon candidates (see page 11). A confirmed exomoon detection can be, thus, within reach in the near future (Lazzoni et al., 2022; Teachey, 2024).

Before we dive into the different exomoon detection methods, it would be beneficial to expand on what exactly can be considered as an exomoon. In the case that one of the two orbiting bodies's mass is significantly lower, like in the case of the Galilean satellites, the answer is straightforward. By convention, if the center of mass of the system is outside of the largest body, the system can be considered a binary system. However,when a smaller body orbits an isolated planet or a brown dwarf (BD), the exact terminology remains uncertain. In addition to that, the line between what can be considered a BD or a planet is blurred, especially between the deuterium-burning limit at $\approx 13M_{Jup}$, below which bodies are often characterized as planets (Teachey, 2024), and the hydrogen-burning limit at $\approx 80M_{Jup}$ (Chabrier et al., 2023), the dividing line between stars and BDs. In this thesis we make use of the term companion and exomoon interchangeably, keeping in mind that the diversity of the worlds can challenge their strict classification.

By studying exoplanets we do not only expand our understanding of distant worlds, but also gain insights into our own. Observations of life on Earth have shown that ecosystems, at the very least, require liquid water, a steady energy source, and a supply of nutrients (Heller et al., 2014). Interestingly, the only bodies in the Solar System that fulfill these habitability requirements apart from the Earth are moons of the gas giant planets. This fact has inspired scientists to move from the conventional planet HZ, to the moon habitability zone, which can significantly increase the potential habitable bodies in the cosmos (Dobos et al., 2017; Heller, 2012). In addition, a moon might play a significant role in making its parent planet inhabited. For example, the Earth's Moon affects tides on Earth, which could have played a role in the development of early life (Benn, 1999).

The explosion of the discovered exoplanets has enabled studies of exoplanet demographics. These indicate that our Solar System might not be very common (Mishra et al., 2023). However, we lack a comparable reference point for moons. Exomoon detections could help shed light into questions such as the prevalence of moons, their properties particularly compared to the Solar System ones, and the rarity of a moon similar to Earth's. In addition, satellites gives us hints on their host planets' formation and dynamical history. For example, the existence and properties of the Galilean moons provide insights on the location of Jupiter's formation and its migration history (Heller et al., 2015). Recently, the existence of an ancient satellite has been proposed to explain the obliquity of Uranus (Saillenfest et al., 2022).

Formation mechanisms

Moon formation is a natural consequence of planet formation (Barr, 2016). Having given several examples of how the existence and properties of moons can affect our interpretation of its host planet formation history, it is now worth exploring the several moon formation theories that have been proposed. The large and regular moons of the gas giants are thought to form in a circumplanetary disk (CPD) of material around the young planet that is accreting gas from the solar nebula, in a similar way that planets form around stars. Satellites formed in this way have orbits that are mostly coplanar with small eccentricity and inclination values. Canup &Ward (2006) suggest that they follow a mass scaling law compared to their hosts of $\approx 10^{-4}$, which is governed by the interplay between the inward delivery of material and the loss of satellites via orbital decay. The latter mass scaling law is in agreement with the mass fractions of the Solar System gas giants' moons.

Another formation scenario, which has been invoked to explain our own Moon is the giant impact scenario (Canup &Asphaug, 2001). Pluto's moon, Charon, is also thought to have formed in this way (Canup, 2010). In the inner Solar System, collisions between planetary embryos frequently occur during the late stages of terrestrial planet formation (Agnor et al., 1999). It is reasonable to assume that terrestrial planets in other systems would also experience similar phenomena. Nakajima et al. (2022) simulated such collisions and found that more massive rocky planets produce a gas-rich disk, which induces drag on moonlets, causing them to return to the planet. This suggests that impacts are more likely to produce fractionally large satellites around less massive rocky exoplanets.

Finally, capture of satellites constitutes a third formation mechanism. The moons formed via this way can be larger than the moons formed in a CPD. Triton, Neptune's largest moon, exhibits orbital characteristics that strongly indicate it was captured (McKinnon et al., 1995). Its retrograde orbit is tilted approximately 157° relative to Neptune's equator, which is indicative of formation via capture. Such an even may have disrupted the original moons of Neptune, assuming one existed prior to the current (Rufu &Canup, 2017).

We will now expand on the different exomoon detection methods that have been proposed, highlighting their respective strengths and limitations in the context of exomoon discovery.

Exomoon detection methods and candidate systems

Searches for extrasolar satellites are providing either constraints on exomoon properties from non-detections, signs of a moon's presence—such as detected volcanic species or gaps in ring systems—or potential candidate systems. A variety of indirect and direct methods have been proposed for exomoon detection. Indirect methods analyze the impact of a moon on a planet's signal. These include centroid shifts (Agol et al., 2015) (Figure 1.4 a) and Doppler monitoring of directly imaged exoplanets resulting from gravitational interactions between the planet and its companion (Vanderburg et al., 2018). Additional detection techniques involve the dynamical sculpting of circumplanetary disks (Kenworthy &Mamajek, 2015). In this thesis, I explain each method with respect to the corresponding exoplanet detection method to make a clear distinction between the possible ways that an exomoon can be found depending on the exoplanet characterization method, and place the following chapters into context. To aid the explanation, Figure 1.5 presents the exoplanet population found as of March 2025, depending on their orbital period and mass. Some Solar System planets, together with exoplanets discussed in this thesis are also shown.

Exomoon detection around transiting exoplanets

Transiting exoplanets make up the majority of detected exoplanets. There is, thus, a variety of methods proposed to detect satellites around them. The first one was proposed by Sartoretti &Schneider (1999), who show that detecting an exomoon transit in the lightcurve of a transiting exoplanet is possible with an observation time equal to the planet's orbital period, provided that the satellite is large enough (Figure 1.4 b). They suggested that even if the satellite transit is itself not detectable, as an additional dip in the star's lightcurve, the presence of a moon can be inferred by the shift of the planet's transit timing (Transit Timing Variation - TTV (Simon et al., 2007)), caused by the motion of the planet around the planet-moon barycenter. With the launch of the Kepler Space Telescope and the subsequent explosion of detected transiting systems, interest in studying exomoons around transiting planets grew significantly. Kipping (2008, 2009) showed that not only the timing of the planet's transit (Transit Duration Variations - TDVs), but also its duration is affected by the presence of an exomoon. The combination of TTVs and TDVs can give the mass and semi-major axis of a putative satellite. A number of papers followed investigating the properties of TTVs/TDVs as a detection method for exomoons (see e.g. Kipping (2020), Heller et al. (2016)a), as well as the first systematic program to search for the satellites of extrasolar planets, namely the Hunt for Exomoons with Kepler (HEK). HEK conducted a photodynamical modeling analysis of approximately 60 planets to search for exomoon signatures (Kipping et al., 2012). However, it was in HEK VI (Teachey et al., 2017) that the authors examined 284 planets to investigate the Orbital Sampling Effect (OSE). OSE appears as a characteristic reduction in flux at the edges of a planetary transit when analyzing a time-averaged, phase-folded lightcurve (Heller, 2014),(Heller et al. (2016)b). Given a sufficient number of planet transits, OSE can be used to identify moons as small as Ganymede. HEK VI yielded one exomoon candidate, Kepler-1625b-i, a putative exomoon with size comparable to that of Neptune (Teachey et al., 2017). Kipping et al. (2022) performed a survey around 70 giant transiting exoplanets with Kepler, and identified the candidate Kepler-1708 b-i. The latter is, similarly to Kepler-1625b-i, quite large, ≈ 2.6 Earth radii.

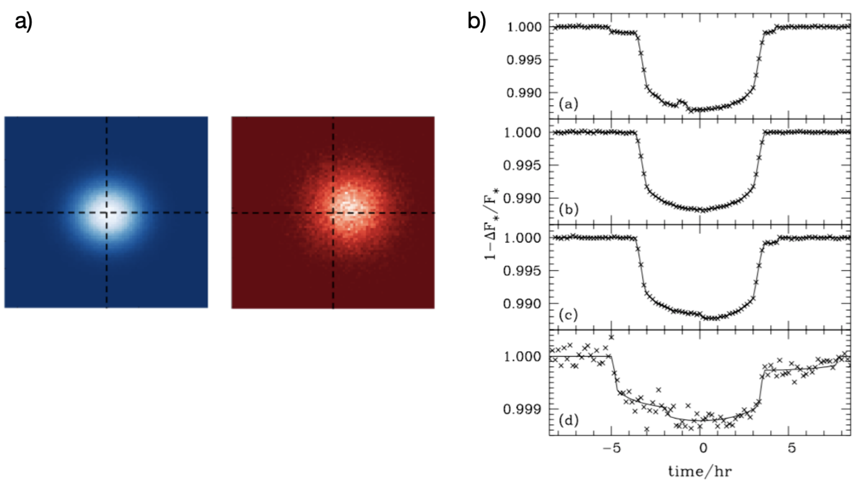

Figure 1.4: Illustrations of two different exomoon detection methods. a) Centroid shifts (Agol et al., 2015): At bluer wavelengths that are dominated by the planet's flux, the centroid aligns with the planet's position. At redder wavelengths that are dominated by a moon, the centroid shifts to the moon's position. b) Exomoon transits (Sartoretti &Schneider, 1999): Several moon transits distinguishable on planet transit lightcurves.

In addition to monochromatic photometric effects, exomoon detection has also been suggested through the spectral analysis of a system. Volcanic material coming from an exomoon similar to Io (exo-Io) can cause detectable signals in the spectrum of a planet (Ben-Jaffel &Ballester, 2014; Gebek &Oza, 2020; Meyer zu Westram et al., 2024). Oza et al. (2019) identified an exomoon candidate around the planet WASP-49b, attributing this to signatures of sodium detected in the planet's transmission spectrum.

Exomoon detection around DI exoplanets

DI has revealed planets at great distances from their host star. This is significant for the hunt of exomoons, as planets further away from their host star are more likely to host moons (Dobos et al., 2021). With DI, the light coming directly from the planet itself can be utilised. This can allow for the direct detection of a companion in wavelengths where the moon is brighter than its host. For example, an Earth-like moon could be brighter than a Jupiter-like planet between 1 and 4 microns, if the latter's atmosphere produces strong methane and water absorption features, suppressing the giant planet's flux in this range (Williams &Knacke, 2004). Direct imaging has given us a candidate that similarly to the two transiting candidates of Teachey et al. (2017) and Kipping et al. (2022) look nothing like the moons of the Solar System. The DI candidate is a 1MJup companion around the low-mass ($10M_{Jup}$) BD DH Tau B (Lazzoni et al., 2020).

Various approaches have been suggested for applying planet detection techniques to the flux of a planet with the goal to reveal exomoons. For instance, radial velocity and astrometry can be utilized (Lazzoni et al., 2022). Additionally, moon transits can be identified through variations in the planet's photometric signal (Cabrera &Schneider, 2007). Although these techniques have not yet yielded promising exomoon candidates, they have helped establish important detection limits. In particular, Vanderburg &Rodriguez (2021) gave the first RV limits of exomoons around HR 8799, which are in the order of Jupiter mass planets. Recently, Ruffio et al. (2023) demonstrated that next-generation high-contrast imaging 30 meter class telescopes combined with spectroscopy will enable the detection of close-in, Solar System-sized moons around nearby brown dwarfs, whereas current-generation telescopes can only identify giant moons, akin to gas giant planets in the Solar System (Vanderburg et al., 2018; Lazzoni et al., 2022; Ruffio et al., 2023; Horstman et al., 2024).

The glare from their host star often obscures directly imaged exoplanets, making exomoon detection difficult with conventional methods. Thus, apart from applying the aforementioned techniques around DI exoplanets or BD around a host, several techniques have been proposed to detect exomoons around isolated planets or BDs (Limbach et al., 2021). Low-period moons can have geometric transit probabilities greater than 10, making their detection more feasible in large-scale surveys. PINES is an ongoing survey aimed at detecting transiting exosatellites around nearly 400 nearby brown dwarfs and free-floating planets (FFPs) (Tamburo et al., 2022a). The survey is capable of identifying exosatellites larger than 2.5 R_{Earth} and has detected a $\approx$5 R_{Earth} candidate orbiting $2MASS\,J0835+1953$ (Tamburo et al., 2022a,b). In addition, Limbach et al. (2024c) studied 44 archival Spitzer lightcurves, with no significant evidence of satellite transits, sensitive to 0.7 R_{Earth} satellites. Limbach et al. (2023) recently introduced the TEMPO survey, a 30-day observation program utilizing the Nancy Grace Roman Space Telescope to search the Orion Nebula Cluster for exomoon transits, with the capability to detect bodies as small as Titan. Finally, Earth-Moon analogs will be detectable for systems within 10 pc with the upcoming HWO (Limbach et al., 2024a).

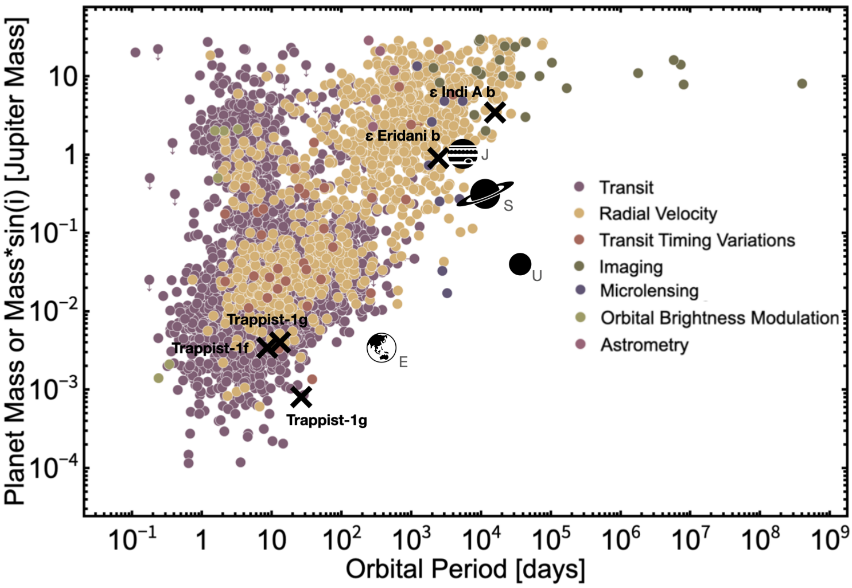

Figure 1.5: A planet mass as a function of orbital period of all the detected exoplanets as of March 2025. Solar System planets are shown on the plot, along with the planets discussed in this thesis. Credit: Adapted from NASA Exoplanet Archive

Exomoon candidates

In this section, I present the exomoon candidates proposed up to 2025, and any controversies surrounding their detection. The candidate systems so far include the following.

1. J1407 b: (Kenworthy &Mamajek, 2015) proposed the presence of putative exomoons from a transit observation of J1407. The transit was linked to a large disk featuring gaps, which were believed to result from the presence of exomoons. Later on it was suggested that J1407 b may not be bound to the star and that it was a free floating system in front of the star (Kenworthy et al., 2020; Mentel et al., 2018).

2. Exomoon candidates found via microlensing, namely MOA-2011-BLG-262 (Bennett et al., 2014), and MOA-2015-BLG-337 (Miyazaki et al., 2018): Detection via microlensing has the disadvantage that observations cannot be repeated. Recently, the MOA-2011-BLG-262 candidate was confirmed to be a low-mass star host with a planet, based on Keck adaptive-optics imaging that directly measured the lens brightness (Terry et al., 2025).

3. Neptune sized moons around transiting gas giants: Kepler-1625 b-i (Teachey &Kipping, 2018) and Kepler-1708 b-i (Kipping et al., 2022) have generated controversy in the literature, with the putative moon signals were found to be fitting (Heller &Hippke, 2024) of data reduction artifacts (Kreidberg et al., 2019). In addition, the

unexpected nature of the candidates themselves has been questioned, particularly regarding their possible formation mechanism (Heller, 2018).

4. WASP-49 b: Sodium absorption observed for the Hot Jupiter WASP-49b was attributed by Oza et al. (2019) to a torus of material that may exist around the host planet. The candidate around WASP-49b remains to be confirmed, as an independent exomoon detection method is needed apart from the indirect method of identifying gases in absorption during the planet's transit. In addition, exomoons around low-period planets are less likely to have stable orbits (Dobos et al., 2021).

5. 2MASS J11193254–1137466 AB: Limbach et al. (2021) claim the detection of a 1.7 R_{Earth} moon transit around an isolated planetary mass object. The data exhibit significant variability with amplitudes similar to those of the suspected transit, and follow-up observations are needed to confirm the presence of the putative moon.

6. W1935: Faherty et al. (2024) detected methane CH_4 in the emission of an isolated BD. The authors claim that this could be associated with a temperature inversion in the upper atmosphere, which can potentially be caused by auroras, linked to nearby moons.

Having discussed the disadvantages that exomoon detection around transiting exoplanets may face, we can shift our interest towards targeting DI exoplanets or IPMOs, given their potential for exomoon detection. Direct imaging of heated exomoons presents challenges, as it requires suppressing the star's light while also accounting for the combined flux from both the moon and its host planet. However, tidally heated exomoons (THEMs) (Limbach &Turner, 2013) can outshine their host planet in certain infrared bands due to tidal interactions between the exomoon and the planet. Unlike other methods such as transits, direct detection through thermal spectral energy distribution (SED) does not depend on a specific satellite orbital phase or require multiple observations. This approach provides a detection window for exomoons orbiting gas giant planets at distances of several tens of astronomical units from their parent star. In this thesis, I discuss possible ways to detect THEMs around DI exoplanets or IPMOs. Firstly, I give an introduction on tidal heating, and its implications for the moons of the Solar System.

1.3 Tides

On Earth we experience the effect of tides; the coastline's level changes as a result of the Moon's gravity. Ocean tides have shaped traditions in different cultures, drive one of the worlds most biodiverse environments, and can even be used for power generation. But what is causing this phenomenon? As the Moon orbits around the Earth it exerts a tidal force on the entire planet. This force varies across the Earth; it is strongest on the side facing the Moon and weakest on the opposite side. This variation creates a deformation, or a "tidal bulge", on opposite sides of the Earth's surface, resulting in high- and low-tides. It also has an effect on the rocky part of the Earth. Such "Terrestrial tides" can cause, for example, volcanic eruptions.

The same phenomenon does not only occur on Earth. It has big implications in other bodies of the Solar System, in exoplanetary systems, and might be an important factor for the emergence of life in other worlds. In the Solar System tidal forces affect the orbits, interior, and surface properties of various bodies, producing different effects on each. Tidal forces are responsible for the geologic activity of Io, the most volcanically active body in the Solar System (Peale et al., 1979). They drive volcanic eruptions, and plumes of material that contribute to the resurfacing that gives Io a young surface (Geissler et al., 2004). The volcanoes of Io are an active field of research and have been mapped and extensively studied (see e.g. de Kleer &de Pater (2016); Bartolić et al. (2022); Davies et al. (2015)). Figure 1.6 a, d both show images of Io's surface, in visible and IR wavelengths, where the excess heat from the volcanoes are clearly distinguishable.

A surprisingly young surface with cracks and ridges (Figure 1.6c) was also discovered at the Jovian moon Europa, when Voyager encountered it (Smith et al., 1979). It was later proposed that a similar mechanism to Io contributes to the geological activity, and that it can prevent the solidification of a subsurface ocean (Cassen et al., 1979). In 2012, the Hubble Space Telescope captured images providing evidence of plumes erupting from the surface of Europa (Saur et al., 2011; Roth et al., 2014). It is now thought that the supposed plumes originate from either water pockets in the ice or from the water ocean. Similarly, Saturn's moon Enceladus is believed to have a subsurface liquid water ocean, maintained by tidal forces, which drive the water vapor geysers erupting from its surface (Figure 1.6b) (Spencer et al., 2018).

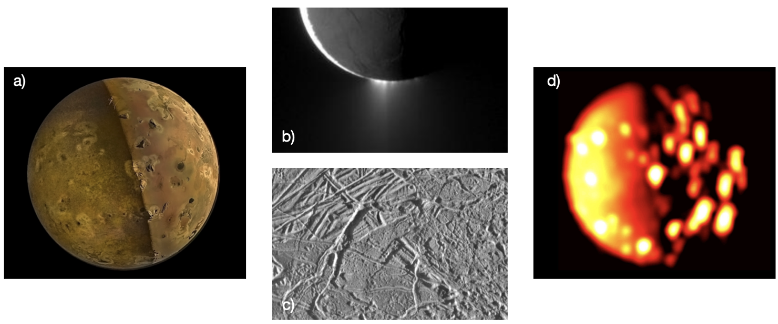

Figure 1.6: Diversity of tidally active moons. a) Image of Io where distinct volcanoes and lava lakes are distinguishable b) Enceladus' plume. Image taken by Cassini Credit:NASA/JPL/Space Science Institute c) Ridges on Europa. Image taken by solid state imaging television camera aboard the Galileo mission Credit: NASA/JPL/University of Arizona Credit: NASA/JPL-Caltech/SwRI/MSSS d) Infrared image of Io's southern hemisphere from data collected by the JIRAM instrument aboard Juno Credit: NASA/JPL-Caltech/SwRI/ASI/INAF/JIRAM

1.3.1 Tides and tidal heating: Basic concepts

Crucially for this thesis, tidal forces can generate heat within the interior of a body. The response of a body to tidal forces depends, among others, on its orbit. When the orbit is elliptical the tidal forces are stronger near periapsis. This results in the tidal bulge to vary over the course of the orbit, as can be seen in Figure 1.7, which in turn generates internal friction heating the interior. The amount of heat that is generated in the interior of a secondary body orbiting a primary depends, among other parameters, on the orbital eccentricity and the semi-major axis of the secondary. In addition to eccentricity driven tides, obliquity tides that arise from the angle between the body's rotational axis and its orbit, can also contribute to tidal dissipation.

The extent of tidal deformation of a body due to tides is parametrized by the Love number k2 (Love, 1911), which measures amplitude of the tidal response. A higher Love number indicates a more deformable interior. Love numbers are typically complex, except in the case of a perfectly elastic body, where the tidal response is instantaneous. On the other hand, when a body is viscous, the tidal response lags behind the tidal force by a phase angle. This lag, caused by internal energy dissipation, is reflected in the phase of the complex Love numbers (Renaud &Henning, 2018). Together with the tidal quality factor Q, which reflects how dissipative the body is, the ratio $\frac{k_2}{Q}$ is a key parameter in models of tidal heating and orbital evolution (see e.g. Dobos &Turner (2015); Renaud &Henning (2018); Rovira-Navarro et al. (2021))).

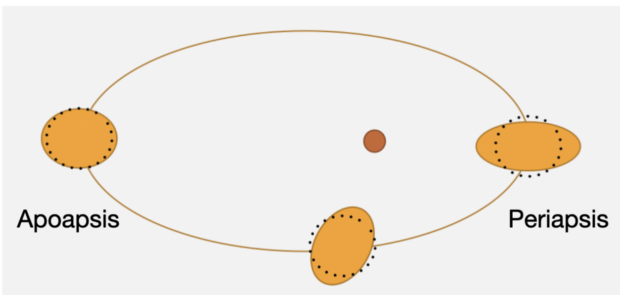

Figure 1.7: Illustration of the tidal bulge evolution throughout an eccentric orbit in a planet-central reference frame. The planet is depected in brown while the moon in yellow. The tidal bulge is exaggerated for clarity.

In a two body system, as the secondary body interacts gravitationally with the primary body, its interior is heated, with the energy coming from its own orbital and rotational energy. The latter leads to tidal circularization in a two-body system, where an initially elliptical orbit gradually becomes circular. The tidal bulge raised on the secondary by the primary drive this circularisation process, as it is misaligned with the line connecting the two bodies, creating torques that remove energy from the orbit, and thus, leading to eccentricity damping (Peale, 1999). Over time, tidal interactions also slow down the rotation of the secondary body until the latter becomes tidally locked. Tidal locking occurs when the secondary's rotational period matches its orbital period. The tides raised on the planet by the satellite can cause orbital migration, which plays a fundamental role in the long-term dynamical evolution of satellite systems. In the case that planet's tidal bulge is ahead the satellite, angular momentum is transferred from the planet's spin to the satellite's orbit, causing the satellite to migrate outward. If the bulge lags behind, the orbit decays inward (Goldreich &Soter, 1966).

In more complex systems gravitational forces from additional bodies can perturb the orbit. Instead of the eccentricity decreasing, orbital circularization is prevented, allowing tidal heating to persist over long timescales. This is what happens, for example, in the case of the Galilean moons of Jupiter. In particular, the moons continuously influence each other through periodic gravitational interactions, distorting their orbits. Ganymede, Europa, and Io are in a 1:2:4 Mean Motion Resonance (MMR); for every four orbits of Io around Jupiter, Europa and Ganymede complete two and one, respectively. This resonance causes the moons to gravitationally perturb each other at regular intervals, maintaining increased orbital eccentricities. It is thus a major factor in sustaining Io's extreme volcanic activity. In addition by preventing Europa's orbit to fully circularize it contributes to the maintainance of its subsurface ocean (Cassen et al., 1979). MMRs have also been observed in several exoplanetary systems, like the Trappist-1 system (Teyssandier et al., 2022). In the context of exomoon detections such resonances do not only contribute in sustaining extreme temperatures, but may also imply the existence of additional, unseen moons, in the case that the observed one is tidally heated.

Under the assumption of zero obliquity, which is a reasonable assumption for Io and other regular satellites (Baland et al., 2012), the tidal heat that is generated in the interior of a satellite follows Equation 1.1 (Segatz et al., 1988; Makarov &Efroimsky, 2014)):

$$\dot{E} = -\frac{21}{2}\mathrm{Im}(k_2)\frac{(nR)^5}{G}e^2, \tag{1.1}$$

where n is the mean motion, e the orbital eccentricity, R the radius of the satellite, and G the universal gravitational constant. $\mathrm{Im}(k_2)$ is the imaginary part of the k_2 Love number and is a parameter that describes the deformation of the gravitational field of a body in response to tides. $Im(k_2)$ depends on the interior structure, its material the orbital period of the satellite (Segatz et al., 1988).

One common approach for modeling tidal dissipation is with the so-called fixed Q model, which is broadly used in tidal calculations, and assumes that $\mathrm{Im}(k_2) = \frac{k_2}{Q}$, and that is constant with respect to the orbital frequency and the thermal state of a satellite (Renaud &Henning, 2018; Henning et al., 2009). In the latter expression Q is the tidal quality factor (Kaula, 1964), and measures the fraction of orbital energy lost to dissipation per orbit as a result of internal friction. The fixed-Q model highly underestimates the tidal heat of the body (see e.g. Ross &Schubert (1989)), and does not take into account Q's dependancy on the satellite's orbital period. In addition, it has been shown that material properties of the interior strongly depend on its temperature (Moore, 2003; Fischer &Spohn, 1990). Unlike the fixed Q model, viscoelastic models incorporate the temperature dependence of the body, taking into account the thermal state of a planet and its response to tidal forces. This allows for a more realistic representation of how the planet's interior responds to tides.

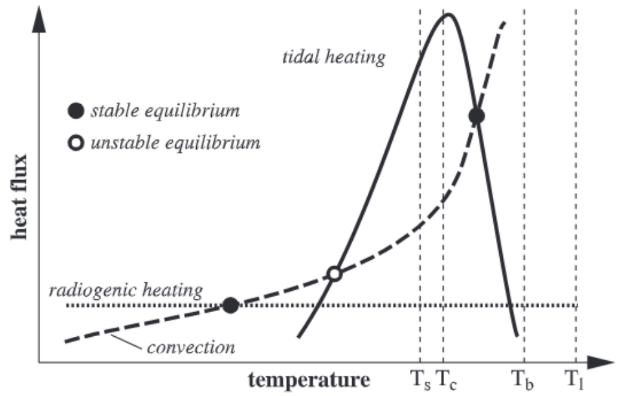

Figure 1.8: Interior heat as a function of mantle temperature. Dashed line: Radiogenic heat Contiguous line: Generated tidal heat. Reference: Moore (2003)

The most simple viscoelastic model is the Maxwell model. Because Im(k_2) is a function of the interior's material properties, namely the rigidity (μ), density (ρ), and viscosity (η), as a result, the generated tidal heat flux also depends on the temperature. As illustrated in Figure 1.8 tidal heat flux (continuous line) reaches its peak at a critical temperature (T_c). Between the solidus (T_s) and liquidus (T_l) temperatures, the material undergoes partial melting. Tidal dissipation increases when the tidal period is near the Maxwell time ($\frac{\eta}{\mu}$). When the forcing period is shorter than the Maxwell time, the body behaves elastically, whereas when the forcing period is greater, the body responds as a viscous fluid. The dashed curve represents the body's convective heat loss. Equilibrium points are marked by circles; for instance, the solid circle between T_c and T_l indicates a stable equilibrium point. If the temperature rises, convective cooling surpasses the tidal heat flux, leading to a temperature decrease. Conversely, if the temperature drops, the tidal heat flux dominates, causing the temperature to rise back to equilibrium.

1.3.2 Probing planetary interiors

Because tidal response depends on the material properties of a body, a connection can be made between the tidal response and the interior structure. For example, the exact interior structure and heat transfer mechanism that takes place in the interior of Io is still unknown; whether Io harbors a shallow, global magma ocean has remained an open question since the discovery of its volcanism. For decades, scientists had speculated that Io's intense tidal heating could be powerful enough to melt a significant portion of its interior, potentially creating a global subsurface magma ocean. Moore (2001) proposed that Io's tidal heat is transported by the advection of melt, for melt fractions of less than 20 percent. There are two end-case scenarios for Io's interior: a partially molten, mostly solid interior, and an interior with a global magma ocean. Measuring Io's tidal response can help shed light into this question. If Io possesses a shallow global magma ocean, its tidal deformation would be larger than in a scenario with a solid, rigid interior, as the decoupling of the liquid layer leads to an enhanced tidal response. Efforts to determine Im(k_2) for Io using astrometric observations (Lainey et al., 2009) have constrained its value to 0.015 ± 0.003. Recently Park et al. (2025) by combining the most recent Juno and previous Galileo Doppler data, constrained Io's k_2, and proposed that a shallow global magma ocean does not exist, and that their results are consistent with Io having a mostly solid mantle.

Similarly, a connection can be made between an exoplanet's tidal response and its interior properties. There has been several papers investigating theoretically the effect of tidal heating on exoplanet systems using a multilayer approach (Barr et al., 2018; Shoji &Kurita, 2014). Henning et al. (2009) gave an extensive overview of the effect of different rheology models and interior properties for exoplanets and their implications on their tidal heating rates. In addition, the effect of tidal heating is expected to be tremendous on exoplanet habitability (Dobos et al., 2019). These studies have paved the way for the detection of exoplanet volcanism, driven by tidal heating (Peterson et al., 2023).

Direct detection of tidally heated exomoons (THEMs), driven by tidal interactions in eccentric, short-period orbits, has been proposed as a method for identifying these bodies (Limbach &Turner, 2013). This process requires the presence of tidal heating within the moon's interior. Most studies examining the direct detection of THEMs have assumed a uniform temperature distribution across the moon's surface to estimate the temperatures achievable through tidal interactions using a multilayer approach (Dobos &Turner, 2015; Rovira-Navarro et al., 2021). Jäger &Szabó (2021) argue that a THEM's temperature distribution is likely to be uneven, with hotspots similar to those seen on Io. They suggested that this uneven temperature distribution could enhance the direct detectability of THEMs.

1.4 This thesis

The work done during this PhD research, aims to investigate the effect of tidal heating in the observability of extra-solar satellites around exoplanets. More particularly, this thesis focuses on the effects of tidal heating on the detectability of exomoons around directly imaged and radial velocity exoplanets, IPMOs or BDs. The main goal is to identify the physical and/or orbital parameters that would make THEMs detectable with different methods and existing or future instruments. In parallel, we also investigate how well the physical properties of potentially detected exomoons might be characterized according to observational and theoretical constraints. The second part of this thesis uses interior models used in the characterization of Solar System moons, to assess potential interior structures of the likely icy planets of the system Trappist-1. We model the tidal heat produced in their interior and identify the thickness and depth of any potential subsurface oceans. We also conclude on the detectability of cryovolcanism in the system.

Chapter 2: Tidally Heated Exomoons around ϵ Eridani b: Observability and prospects for characterization

We begin with Chapter 2, where we explore the possibility of detecting THEMs in IR wavelengths with JWST. We study as an archetype the system ϵ Eridani b, a nearby system with a distance of 3.2 parsec (see also Figure 1.2). We firstly, model exomoons of different size for a range of orbital parameters, and conclude on the ones that would make them detectable. To do so, we modelled a radially symmetric, spherical body in which heat moves through magma advection in a partially molten layer and convection in the deeper mantle. We used a combined thermal and tidal model to identify stable equilibrium states where tidal heating balances internal heat transport within a moon. To evaluate detectability with MIRI, we accounted for uncertainties in both the interior composition and tidal dissipation parameters, analyzing the proportion of simulated moons that would exhibit observable signatures. We find that for comparable semi-major axes and eccentricities with the satellites of the Solar System gas giants, Mars-sized exomoons or larger would be detectable.

Chapter 3: The spectroastrometric detectability of nearby Solar System-like exomoons

We continue with Chapter 3, which explores the detectability of THEMs around exoplanets with the method of spectroastrometry. Spectroastrometry uses the spectral variation of the center of light as a result of an exomoons orbit. We derive an analytic expression for the signal, and apply this on the detection of THEMs around exoplanets. We determine the temperatures of THEMs that can be detected with the upcoming ELT, using ϵ Indi Ab as an archetype. We find that the ELT will be able to detect exomoons comparable in size to the Solar System moons of moderate temperatures. In addition, Mars-sized icy moons can be detected in nearby systems with the method of spectroastroemtry. Thus, with this method we are sensitive to much colder exomoons with temperatures that are closer to those of Solar System satellites.

Chapter 4: Direct detectability of tidally heated exomoons by photometric orbital modulation

In Chapter 4 we model the effect of hotspots, like the ones observed on Io, on the detectability of THEMs, deviating from the assumption of a uniformly distributed surface temperature, that was taken in the two previous chapters. We introduce the method of photometric orbital modulation for the detection of THEMs. As a moon orbits its host, inhomogeneously distributed volcanic features or hotspots cause a photometric variability on the signal of a planet-moon system. The periodicity of this signal introduces a distinct feature in the frequency domain of the system's time-variable flux. In this Chapter, we investigate the properties of THEMs that would make them observable with JWST around IMPOs. For Mars-sized exomoons, this applies to system distances of up to 10 pc, while Earth-sized exomoons can be detected at even greater distances. Io-sized exomoons may be detectable in extremely close systems, and when hotspot temperatures are on the higher end of the spectrum of the assumed temperatures. Notably, this approach is applicable to non-transiting orbital inclinations, and thus, expands the range of detectable exomoons around IPMOs.

Chapter 5: Modeling the interiors of Trappist-1f, g, h: Tidal Heating, Subsurface Oceans, and Cryovolcanic Activity

We finish the scientific part of this thesis with Chapter 5, where we expand our research on extrasolar volcanism, focusing this time on potentially icy exoplanets. In this Chapter we investigate the internal heating of Trappist-1f,g, and h, and its effect on the thermal state of their interior. We use models previously used to describe the thermal structure and heat generation on Solar System icy moons, and draw conclusions on the equilibrium thermal states of the planets. We find that if the Trappist-1f and h planets have a subsurface water ocean underneath, they likely posses a thin ice shell, with thicknesses between ≈ 4 and 10 km. We also explore whether the internal heat generation is sufficient to drive detectable cryovolcanic activity. We do so for a configuration where the outgassing is evenly distributed over the surface, and one where gayser-like plumes are concentrated at one pole of the planet. The most optimistic volcanic configurations would require a JWST campaign lasting over a decade. We suggest that the community focus on exploring other planets to observe cryovolcanic activity.

I conclude this introduction with an outlook on the future of exomoon detection. Although no exomoon detection has been confirmed yet, the field of exoplanet research has advanced rapidly over the past decades. Cycle 3 of JWST has included proposals aimed at detecting exomoons; one around a long-period Kepler planet (Cassese et al., 2024), and an Earth-Moon analogue (Pass et al., 2024). With the next generation of telescopes and improved modeling techniques, we may soon achieve exomoon detections. However, it may take some time until the field of exomoons becomes as fruitful in discoveries and as routine as exoplanet detections are today. The path of discovery is hard to predict, and the diversity of worlds that may be revealed in the future might surprise us, and exceed our expectations, if past discoveries are any indication. In any case, detecting and characterizing exomoons will have a profound impact, as we will gain new insights of planetary systems and the potential for life beyond Earth.

Bibliography

Agnor, C. B., Canup, R. M., & Levison, H. F. 1999, Icarus, 142, 219, doi: 10.1006/icar.1999.6201

Agol, E., Jansen, T., Lacy, B., Robinson, T. D., & Meadows, V. 2015, The Astrophysical Journal, 812, 5, doi: 10.1088/0004-637X/812/1/5

Ahrer, E.-M., Alderson, L., Batalha, N. M., et al. 2023, Nature, 614, 649, doi: 10.1038/s41586-022-05269-w

Baland, R.-M., Yseboodt, M., & van Hoolst, T. 2012, Icarus, 220, 435, doi: 10.1016/j.icarus.2012.05.020

Barr, A. C. 2016, Astronomical Review, 12, 24, doi: 10.1080/21672857.2017.1279469

Barr, A. C., Dobos, V., & Kiss, L. L. 2018, AA, 613, A37, doi: 10.1051/0004-6361/201731992

Bartolić, F., Luger, R., Foreman-Mackey, D., Howell, R. R., & Rathbun, J. A. 2022, The Planetary Science Journal, 3, 67, doi: 10.3847/PSJ/ac2a3e

Ben-Jaffel, L., & Ballester, G. E. 2014, The Astrophysical Journal Letters, 785, L30, doi: 10.1088/2041-8205/785/2/L30

Benisty, M., Bae, J., Facchini, S., et al. 2021, The Astrophysical Journal Letters, 916, L2, doi: 10.3847/2041-8213/ac0f83

Benn, C. R. 1999, Earth, Moon, and Planets, 85, 61, doi: 10.1023/A:1017082925182

Bennett, D. P., Batista, V., Bond, I. A., et al. 2014, The Astrophysical Journal, 785, 155, doi: 10.1088/0004-637X/785/2/155

Bohn, A. J., Kenworthy, M. A., Ginski, C., et al. 2020, The Astrophysical Journal Letters, 898, L16, doi: 10.3847/2041-8213/aba27e

Borucki, W. J., Koch, D., Basri, G., et al. 2010, Science, 327, 977, doi: 10.1126/science.1185402

Cabrera, J., & Schneider, J. 2007, in Astronomical Society of the Pacific Conference Series, Vol. 366, Transiting Extrapolar Planets Workshop, ed. C. Afonso, D. Weldrake, & T. Henning, 242

Canup, R. M. 2010, The Astronomical Journal, 141, 35, doi: 10.1088/0004-6256/141/2/35

Canup, R. M., & Asphaug, E. 2001, Nature, 412, 708, doi: 10.1038/35089010

Canup, R. M., & Ward, W. R. 2006, Nature, 441, 834, doi: 10.1038/nature04860

Cassen, P., Reynolds, R. T., & Peale, S. J. 1979, Geophysical Research Letters, 6, 731, doi: https://doi.org/10.1029/GL006i009p00731

Cassese, B., Batygin, K., Chachan, Y., et al. 2024, Revealing the Oblateness and Satellite System of an Extrasolar Jupiter Analog, JWST Proposal. Cycle 3, ID. #6491

Cassidy, T. A., Mendez, R., Arras, P., Johnson, R. E., & Skrutskie, M. F. 2009, The Astrophysical Journal, 704, 1341, doi: 10.1088/0004-637X/704/2/1341

Chabrier, G., Baraffe, I., Phillips, M., & Debras, F. 2023, AA, 671, A119, doi: 10.1051/0004-6361/202243832

Chauvin, G. 2024, Comptes Rendus. Physique, 24, 129–150, doi: 10.5802/crphys.139

Cloutier, R. 2024, Exoplanet Demographics: Physical and Orbital Properties. https://arxiv.org/abs/2409.13062

Davies, A. G., Veeder, G. J., Matson, D. L., & Johnson, T. V. 2015, Icarus, 262, 67, doi: https://doi.org/10.1016/j.icarus.2015.08.003

de Kleer, K., & de Pater, I. 2016, Icarus, 280, 378, doi: https://doi.org/10.1016/j.icarus.2016.06.019

Dobos, V., Barr, A. C., & Kiss, L. L. 2019, AA, 624, A2, doi: 10.1051/0004-6361/201834254

Dobos, V., Charnoz, S., Pál, A., Roque-Bernard, A., & Szabó, G. M. 2021, Publications of the Astronomical Society of the Pacific, 133, 094401, doi: 10.1088/1538-3873/abfe04

Dobos, V., Heller, R., & Turner, E. L. 2017, AA, 601, A91, doi: 10.1051/0004-6361/201730541
Dobos, V., & Turner, E. L. 2015, The Astrophysical Journal, 804, 41, doi: 10.1088/0004-637x/804/1/41
Dougherty, M. K., Khurana, K. K., Neubauer, F. M., et al. 2006, Science, 311, 1406, doi: 10.1126/science.1120985
Endl, M., & Cochran, W. D. 2007, in Encyclopedia of the Solar System (Second Edition), second edition edn., ed. L.-A. McFadden, P. R. Weissman, & T. V. Johnson (San Diego: Academic Press), 887–902, doi: https://doi.org/10.1016/B978-012088589-3/50051-7
Espinoza-Retamal, J. I., Zhu, W., & Petrovich, C. 2023, The Astronomical Journal, 166, 231, doi: 10.3847/1538-3881/ad00b9
Faherty, J. K., Burningham, B., Gagné, J., et al. 2024, Nature, 628, 511, doi: 10.1038/s41586-024-07190-w
Feng, F., Tuomi, M., & Jones, H. R. A. 2018, Detection of the closest Jovian exoplanet in the Epsilon Indi triple system. https://arxiv.org/abs/1803.08163
Fischer, H.-J., & Spohn, T. 1990, Icarus, 83, 39, doi: https://doi.org/10.1016/0019-1035(90)90005-T
Fox, C., & Wiegert, P. 2020, Monthly Notices of the Royal Astronomical Society, 501, 2378, doi: 10.1093/mnras/staa3743
Gebek, A., & Oza, A. V. 2020, Monthly Notices of the Royal Astronomical Society, 497, 5271, doi: 10.1093/mnras/staa2193
Geissler, P., McEwen, A., Phillips, C., Keszthelyi, L., & Spencer, J. 2004, Icarus, 169, 29, doi: https://doi.org/10.1016/j.icarus.2003.09.024
Gillon, M., Triaud, A. H. M. J., Demory, B.-O., et al. 2017, Nature, 542, 456, doi: 10.1038/nature21360
Goldreich, P., & Soter, S. 1966, Icarus, 5, 375, doi: https://doi.org/10.1016/0019-1035(66)90051-0
Haffert, S. Y., Bohn, A. J., de Boer, J., et al. 2019, Nature Astronomy, 3, 749–754, doi: 10.1038/s41550-019-0780-5
Hatzes, A. P., Cochran, W. D., McArthur, B., et al. 2000, The Astrophysical Journal, 544, L145, doi: 10.1086/317319
Heller, R. 2012, AA, 545, L8, doi: 10.1051/0004-6361/201220003
Heller, R. 2014, ApJ, 787, 14, doi: 10.1088/0004-637X/787/1/14
Heller, R. 2018, AA, 610, A39, doi: 10.1051/0004-6361/201731760
Heller, R., & Hippke, M. 2024, Nature Astronomy, 8, 193, doi: 10.1038/s41550-023-02148-w
Heller, R., Hippke, M., & Jackson, B. 2016, ApJ, 820, 88, doi: 10.3847/0004-637X/820/2/88
Heller, R., Hippke, M., Placek, B., Angerhausen, D., & Agol, E. 2016, AA, 591, A67, doi: 10.1051/0004-6361/201628573
Heller, R., Marleau, G.-D., & Pudritz, R. E. 2015, AA, 579, L4, doi: 10.1051/0004-6361/201526348
Heller, R., Williams, D., Kipping, D., et al. 2014, Astrobiology, 14, 798–835, doi: 10.1089/ast.2014.1147
Helling, C. 2019, Annual Review of Earth and Planetary Sciences, 47, 583, doi: https://doi.org/10.1146/annurev-earth-053018-060401
Henning, W. G., O'Connell, R. J., & Sasselov, D. D. 2009, The Astrophysical Journal, 707, 1000–1015, doi: 10.1088/0004-637x/707/2/1000
Horstman, K., Ruffio, J.-B., Batygin, K., et al. 2024, RV measurements of directly imaged brown dwarf GQ Lup B to search for exo-satellites. https://arxiv.org/abs/2408.10299
Jäger, Zoltán, J., & Szabó, G. M. 2021, Monthly Notices of the Royal Astronomical Society, 508, 5524, doi: 10.1093/mnras/stab2955

Kaula, W. M. 1964, Reviews of Geophysics, 2, 661, doi: https://doi.org/10.1029/RG002i004p00661

Kenworthy, M. A., & Mamajek, E. E. 2015, The Astrophysical Journal, 800, 126, doi: 10.1088/0004-637x/800/2/126

Kenworthy, M. A., Klaassen, P. D., Min, M., et al. 2020, Astronomy & Astrophysics, 633, A115, doi: 10.1051/0004-6361/201936141

Khurana, K. K., Kivelson, M. G., Stevenson, D. J., et al. 1998, Nature, 395, 777, doi: 10.1038/27394

Kipping, D. 2020, Monthly Notices of the Royal Astronomical Society, 500, 1851–1857, doi: 10.1093/mnras/staa3398

Kipping, D., Bryson, S., Burke, C., et al. 2022, Nature Astronomy, 6, 367, doi: 10.1038/s41550-021-01539-1

Kipping, D. M. 2008, Monthly Notices of the Royal Astronomical Society, 392, 181, doi: 10.1111/j.1365-2966.2008.13999.x

—. 2009, Monthly Notices of the Royal Astronomical Society, 396, 1797, doi: 10.1111/j.1365-2966.2009.14869.x

Kipping, D. M., Bakos, G. , Buchhave, L., Nesvorný, D., & Schmitt, A. 2012, The Astrophysical Journal, 750, 115, doi: 10.1088/0004-637x/750/2/115

Kreidberg, L., Luger, R., & Bedell, M. 2019, The Astrophysical Journal Letters, 877, L15, doi: 10.3847/2041-8213/ab20c8

Lainey, V., Arlot, J.-E., Karatekin, O., & Van Hoolst, T. 2009, Nature, 459, 957—959, doi: 10.1038/nature08108

Lazzoni, C., Desidera, S., Gratton, R., et al. 2022, Monthly Notices of the Royal Astronomical Society, 516, 391, doi: 10.1093/mnras/stac2081

Lazzoni, C., Zurlo, A., Desidera, S., et al. 2020, AA, 641, A131, doi: 10.1051/0004-6361/201937290

Limbach, M. A., Lustig-Yaeger, J., Vanderburg, A., et al. 2024a, Exomoons Exorings with the Habitable Worlds Observatory I: On the Detection of Earth-Moon Analog Shadows Eclipses. https://arxiv.org/abs/2405.02408

—. 2024b, Exomoons Exorings with the Habitable Worlds Observatory I: On the Detection of Earth-Moon Analog Shadows Eclipses. https://arxiv.org/abs/2405.02408

Limbach, M. A., & Turner, E. L. 2013, The Astrophysical Journal, 769, 98, doi: 10.1088/0004-637X/769/2/98

Limbach, M. A., Vos, J. M., Vanderburg, A., & Dai, F. 2024c, The Astronomical Journal, 168, 54, doi: 10.3847/1538-3881/ad4ed5

—. 2024d, Occurrence Rates of Exosatellites Orbiting 3-30M_{Jup} Hosts from 44 Spitzer Light Curves. https://arxiv.org/abs/2405.08116

Limbach, M. A., Vos, J. M., Winn, J. N., et al. 2021, The Astrophysical Journal Letters, 918, L25, doi: 10.3847/2041-8213/ac1e2d

Limbach, M. A., Soares-Furtado, M., Vanderburg, A., et al. 2023, Publications of the Astronomical Society of the Pacific, 135, 014401, doi: 10.1088/1538-3873/acafa4

Love, A. E. H. 1911, Some Problems of Geodynamics (Cambridge University Press)

Makarov, V. V., & Efroimsky, M. 2014, The Astrophysical Journal, 795, 7, doi: 10.1088/0004-637X/795/1/7

Marois, C., Zuckerman, B., Konopacky, Q. M., Macintosh, B., & Barman, T. 2010, Nature, 468, 1080, doi: 10.1038/nature09684

Martins, Z., Bunce, E. J., Grasset, O., et al. 2025, in Proceedings of the VIII Iberian Congress on Planetary Sciences and Solar System Exploration, 35

Mayor, M., & Queloz, D. 1995, Nature, 378, 355, doi: 10.1038/378355a0

McKinnon, W. B. 2015, Geophysical Research Letters, 42, 2137, doi: https://doi.org/10.1002/2015GL063384
McKinnon, W. B., Lunine, J. I., & Banfield, D. 1995, in Neptune and Triton, ed. D. P. Cruikshank, M. S. Matthews, & A. M. Schumann, 807–877
Mentel, R. T., Kenworthy, M. A., Cameron, D. A., et al. 2018, AA, 619, A157, doi: 10.1051/0004-6361/201834004
Meyer zu Westram, M., Oza, A. V., & Galli, A. 2024, Journal of Geophysical Research: Planets, 129, e2023JE007935, doi: https://doi.org/10.1029/2023JE007935
Mishra, L., Alibert, Y., Udry, S., & Mordasini, C. 2023, AA, 670, A68, doi: 10.1051/0004-6361/202243751
Miyazaki, S., Sumi, T., Bennett, D. P., et al. 2018, AJ, 156, 136, doi: 10.3847/1538-3881/aad5ee
Moore, W. B. 2001, Icarus, 154, 548, doi: https://doi.org/10.1006/icar.2001.6739
—. 2003, Journal of Geophysical Research: Planets, 108, doi: https://doi.org/10.1029/2002JE001943
Morabito, L. A. 2012, Discovery of Volcanic Activity on Io. A Historical Review. https://arxiv.org/abs/1211.2554
Nakajima, M., Genda, H., Asphaug, E., & Ida, S. 2022, Nature Communications, 13, 568, doi: 10.1038/s41467-022-28063-8
NASA Planetary Data System. 2025, Planetary Fact Sheet, NASA Goddard Space Flight Center. Accessed 2025-04-04. https://nssdc.gsfc.nasa.gov/planetary/factsheet/
National Academies of Sciences, E., & Medicine. 2023, Origins, Worlds, and Life: A Decadal Strategy for Planetary Science and Astrobiology 2023-2032 (Washington, DC: The National Academies Press), doi: 10.17226/26522
Nogueira, P. H., Lazzoni, C., Zurlo, A., et al. 2024, Astrometric and photometric characterization of η Tel B combining two decades of observations. https://arxiv.org/abs/2405.04723
Oza, A. V., Johnson, R. E., Lellouch, E., et al. 2019, The Astrophysical Journal, 885, 168, doi: 10.3847/1538-4357/ab40cc
Park, R. S., Jacobson, R. A., & Gomez Casajus, L. e. a. 2025, Nature, 638, 69, doi: 10.1038/s41586-024-08442-5
Pass, E., Bean, J. L., Charbonneau, D., Cherubim, C., & Garcia-Mejia, J. 2024, A Search for Exoplanet Satellites that are the Same Size as the Earth's Moon, JWST Proposal. Cycle 3, ID. #6193
Peale, S. J. 1999, Annual Review of Astronomy and Astrophysics, 37, 533, doi: 10.1146/annurev.astro.37.1.533
Peale, S. J., Cassen, P., & Reynolds, R. T. 1979, Science, 203, 892, doi: 10.1126/science.203.4383.892
Peterson, M. S., Benneke, B., Collins, K., et al. 2023, Nature, 617, 701, doi: 10.1038/s41586-023-05934-8
Renaud, J. P., & Henning, W. G. 2018, The Astrophysical Journal, 857, 98, doi: 10.3847/1538-4357/aab784
Ricker, G. R., Winn, J. N., Vanderspek, R., et al. 2015, Journal of Astronomical Telescopes, Instruments, and Systems, 1, 014003, doi: 10.1117/1.JATIS.1.1.014003
Roccetti, G., Grassi, T., Ercolano, B., et al. 2023, International Journal of Astrobiology, 22, 317–346, doi: 10.1017/S1473550423000046
Ross, M., & Schubert, G. 1989, Icarus, 78, 90, doi: https://doi.org/10.1016/0019-1035(89)90071-7
Roth, L., Saur, J., Retherford, K. D., et al. 2014, Science, 343, 171, doi: 10.1126/science.1247051

Rovira-Navarro, M., van der Wal, W., Steinke, T., & Dirkx, D. 2021, 2, 119, doi: 10.3847/psj/abf6cb

Ruffio, J.-B., Horstman, K., Mawet, D., et al. 2023, The Astronomical Journal, 165, 113, doi: 10.3847/1538-3881/acb34a

Rufu, R., & Canup, R. M. 2017, The Astronomical Journal, 154, 208, doi: 10.3847/1538-3881/aa9184

Saillenfest, M., Rogoszinski, Z., Lari, G., et al. 2022, AA, 668, A108, doi: 10.1051/0004-6361/202243953

Sartoretti, P., & Schneider, J. 1999, A&AS, 134, 553, doi: 10.1051/aas:1999148

Saur, J., Feldman, P. D., Roth, L., et al. 2011, The Astrophysical Journal, 738, 153, doi: 10.1088/0004-637X/738/2/153

Segatz, M., Spohn, T., Ross, M. N., & Schubert, G. 1988, Icarus, 75, 187, doi: 10.1016/0019-1035(88)90001-2

Shoji, D., & Kurita, K. 2014, ApJ, 789, 3, doi: 10.1088/0004-637X/789/1/3

Simon, A., Szatmáry, K., & Szabó, G. M. 2007, AA, 470, 727, doi: 10.1051/0004-6361:20066560

Smith, B. A., Soderblom, L. A., Johnson, T. V., et al. 1979, Science, 204, 951, doi: 10.1126/science.204.4396.951

Snellen, I., de Kok, R., Birkby, J. L., et al. 2015, A&A, 576, A59, doi: 10.1051/0004-6361/201425018

Soderlund, K. M., Rovira-Navarro, M., Le Bars, M., Schmidt, B. E., & Gerkema, T. 2024, Annual Review of Marine Science, 16, 25, doi: https://doi.org/10.1146/annurev-marine-040323-101355

Spencer, J. R., Nimmo, F., Ingersoll, A. P., et al. 2018, in Enceladus and the Icy Moons of Saturn, ed. P. M. Schenk, R. N. Clark, C. J. A. Howett, A. J. Verbiscer, & J. H. Waite (University of Arizona Press), 163, doi: 10.2458/azu_uapress_9780816537075-ch008

Suárez Mascareño, A., González-Álvarez, E., Zapatero Osorio, M. R., et al. 2023, A&A, 670, A5, doi: 10.1051/0004-6361/202244991

Tamburo, P., Muirhead, P. S., McCarthy, A. M., et al. 2022a, The Astronomical Journal, 163, 253, doi: 10.3847/1538-3881/ac64aa

—. 2022b, The Astronomical Journal, 164, 252, doi: 10.3847/1538-3881/ac9a52

Teachey, A. 2024, Detecting and Characterizing Exomoons and Exorings (Handbook of Exoplanets, 2nd Edition). https://arxiv.org/abs/2401.13293

Teachey, A., & Kipping, D. M. 2018, Science Advances, 4, eaav1784, doi: 10.1126/sciadv.aav1784

Teachey, A., Kipping, D. M., & Schmitt, A. R. 2017, The Astronomical Journal, 155, 36, doi: 10.3847/1538-3881/aa93f2

Terrile, R. J., & Cook, A. F. 1981, in Lunar and Planetary Science XII, Supplement A. Satellites of Saturn. Abstracts Presented at a Session of the Twelfth Lunar and Planetary Conference, Vol. LPI Contribution 428 (3303 Nasa Road 1, Houston, TX 77058: Lunar and Planetary Institute), 10

Terry, S. K., Beaulieu, J.-P., Bennett, D. P., et al. 2025, The Astronomical Journal, 169, 131, doi: 10.3847/1538-3881/ad9b0f

Teyssandier, Libert, A.-S., & Agol, E. 2022, A&A, 658, A170, doi: 10.1051/0004-6361/202142377

Tobie, G., Mocquet, A., & Sotin, C. 2005, Icarus, 177, 534, doi: https://doi.org/10.1016/j.icarus.2005.04.006

Tsiaras, A., Waldmann, I. P., Tinetti, G., Tennyson, J., & Yurchenko, S. N. 2019, Nature Astronomy, 3, 1086, doi: 10.1038/s41550-019-0878-9

Van Hoolst, T., Tobie, G., Vallat, C., et al. 2024, Space Science Reviews, 220, 54, doi: 10.1007/s11214-024-01085-y

Vanderburg, A., Rappaport, S. A., & Mayo, A. W. 2018, The Astronomical Journal, 156, 184, doi: 10.3847/1538-3881/aae0fc

Vanderburg, A., Rappaport, S. A., & Mayo, A. W. 2018, AJ, 156, 184, doi: 10.3847/1538-3881/aae0fc

Vanderburg, A., & Rodriguez, J. E. 2021, The Astrophysical Journal Letters, 922, L2, doi: 10.3847/2041-8213/ac33b4

Williams, D., & Knacke, R. 2004, Astrobiology, 4, 400, doi: 10.1089/ast.2004.4.400

Wolszczan, A., & Frail, D. A. 1992, Nature, 355, 145, doi: 10.1038/355145a0

Yahalomi, D. A., Kipping, D., Agol, E., & Nesvorny, D. 2024, The Exoplanet Edge: Planets Don't Induce Observable TTVs Faster than Half their Orbital Period. https://arxiv.org/abs/2411.09752